Physical Mechanism of Sono-Fenton Process

Sankar Chakma and Vijayanand S. Moholkar
Dept. of Chemical Engineering, Indian Institute of Technology Guwahati, Guwahati 781 039, Assam, India

DOI 10.1002/aic.14150
Published online July 10, 2013 in Wiley Online Library (wileyonlinelibrary.com)

Hybrid advanced oxidation processes (AOPs), where two or more AOPs are applied simultaneously, are known to give effective degradation of recalcitrant organic pollutants. This article attempts to discern the physical mechanism of the hybrid sono-Fenton process with identification of links between individual mechanism of the sonolysis and Fenton process. An approach of coupling experimental results with simulations of cavitation bubble dynamics has been adopted for two textile dyes as model pollutants. Fenton process is revealed to have greater contribution than sonolysis in the overall decolorization of both dyes. H_2O_2 added to the liquid medium as a Fenton reagent scavenges $^{\bullet}OH$ radicals produced by cavitation bubbles. Addition of only H_2O_2 to the medium during sonolysis does not yield marked difference in decolorization. Elimination of transient cavitation with application of elevated static pressure to the medium does not alter the extent of decolorization. The synergy between sonolysis and Fenton process is, thus, revealed to be negative. The dissolved oxygen in the medium is found to play an important role in decolorization through conservation of oxidizing radicals. © 2013 American Institute of Chemical Engineers *AIChE J,* 59: 4303–4313, 2013
Keywords: fenton process, advanced oxidation process, cavitation, sonolysis, decolorization

Introduction

Use of synthetic organic dyes by the textile industries has increased significantly in recent years and many of these dyes are toxic organic pollutants. Based on their chemical structure, the synthetic dyes are categorized into various classes like acidic, basic, azo, nonazo etc. Among these classes, use of azo dyes has been the maximum (~70%).[1] These dyes appear in the wastewater discharge from textile industries. The degradation (or decolorization) of these dyes using conventional biological techniques is very difficult due to their complex structure. Globally, approximately 10,000 types of dyes and pigments are produced annually, and about 20% of these are discharged as textile industrial effluents without any pretreatment. For the effective decolorization of the synthetic dyes, advanced oxidation processes (AOPs) have been widely employed as alternative methods. These techniques include Fenton, ozonation, photocatalytic techniques, peroxide treatment, sonolysis, enzyme treatments, etc. Literature published in the last decade includes more than 100 papers that report the use of these techniques for decolorization of textile wastewater, containing a wide range of dyes belonging to the different classes mentioned previously. For further boosting, the efficiency of AOPs, hybrid methods have also been widely used that simultaneously employ two or more AOPs mentioned previously and voluminous literature has also been published in this area in the past decade. The combinations of AOPs that have been used includes sono-Fenton, sono-photocatalysis, sono-enzymatic treatments, photo-Fenton techniques, UV/H_2O_2, UV/ozone, ozone/H_2O_2, etc.[2–5] An excellent review of the individual as well as hybrid AOP techniques for treatment of wastewater has been given by Gogate and Pandit.[6,7] The hybrid techniques have been reported to enhance the decolorization kinetics as well as yield. Most of the literature in the area of hybrid AOPs is focused on results than rationale. Although in many articles an attempt is made to quantify the enhancement factor for the decolorization (or degradation) with reference to one of the AOPs, only a few studies have attempted to deduce the exact mechanism of the synergism between the individual AOP. In this article, we have addressed this basic issue in the context of a widely used hybrid AOP, i.e., sono-Fenton process. Several recent articles report employment of sono-Fenton processes for degradation of different organic pollutants.[8–19] We have used two dyes, viz. Acid red B (an azo dye, abbreviated hereafter as ARB) and Blue HE2R (a non-azo dye, abbreviated hereafter as BLH), as model pollutants in this study in view of the large pollution generated by effluent from textile industry, as mentioned earlier. Our approach for identifying the mechanism of the synergism between sonolysis and Fenton process is twofold, i.e., to couple experiments with simulations of cavitation bubble dynamics. In the next section, we present our contemplations and conjectures, on which the methodology and protocols of this study are based.

Contemplations and Conjectures

The degradation (or oxidation or decolorization) efficiency of an advanced oxidation process such as sonolysis or

Additional Supporting Information may be found in the online version of this article.

Correspondence concerning this article should be addressed to V. S. Moholkar at vmoholkar@iitg.ac.in.

Fenton reagent is characterized by the production of $^{\bullet}OH$ radical, which is a powerful oxidizing agent with an oxidation potential of 2.33 V. The $^{\bullet}OH$ radicals are extremely reactive species, and the typical rate constant of their reaction with organic compounds ranges between 10^6-10^9 mol^{-1} s^{-1}.[20] However, the basic mechanism (either physical or chemical) through which $^{\bullet}OH$ radicals are produced in these techniques is completely different. In sonolysis, the radicals are produced through transient cavitation, which is a phenomenon comprising essentially of three phases, viz. nucleation, growth and an adiabatic implosive collapse of a gas or vapor bubble.[21] These phases are driven by pressure variation induced in the liquid medium (or solvent) due to propagation of the ultrasound wave. Gas pockets trapped in the crevices of solid boundaries of the reaction system constitute the nuclei for cavitation. The growth of the bubble is accompanied by evaporation of large amount of solvent at the bubble interface (or bubble wall), and diffusion of solvent vapor toward the core of the bubble. During the ensuing collapse phase, not all of the vapor molecules can diffuse back to the bubble wall and condense.[22] A significant fraction of vapor remains inside the bubble when the bubble motion reaches extremely fast during the final moments of compression. The bubble collapse occurs within as small time as 50 ns, and it is almost adiabatic. The temperature and pressure condition inside the bubble reaches extreme, typically excessive of 5000 K and 500 bar, respectively.[23,24] The entrapped solvent vapor inside the bubble is subjected to these extreme conditions and undergoes thermal dissociation resulting in very many chemical species, some of which are radical species. The solvent used in majority of the sonochemical processes is water, and 8 species could result out of thermal dissociation of water, viz. H_2, O_2, H_2O_2, O_3, $^{\bullet}OH$, $H^{\bullet}$, $O^{\bullet}$, $HO_2^{\bullet}$. The predominant radical species is $^{\bullet}OH$.[22–24] As the bubble reaches minimum radius during the radial motion, these species can either diffuse out of the bubble, or with fragmentation of the bubble these get released and mixed into the medium.

$^{\bullet}OH$ radical production through Fenton process is known to occur through the well-known reactions as follows[20]

$$Fe^{2+} + H_2O_2 \rightarrow Fe^{3+} + OH^- + HO^{\bullet}$$
$$Fe^{3+} + H_2O_2 \rightarrow Fe^{2+} + HO_2^{\bullet} + H^+$$
$$Fe^{3+} + HO_2^{\bullet} \rightarrow Fe^{2+} + O_2 + H^+$$

When the techniques of sonolysis and Fenton are applied together, there are several means through which they can assist/oppose each other's mechanism. One obvious mechanism through which the two AOPs can interact is the formation and utilization of $^{\bullet}OH$ radicals. These radicals are formed at the location of bubble collapse and can independently decolorize the dye molecules. However, being extremely reactive, these radicals do not penetrate or diffuse through the bulk medium. If the concentration of pollutant in the solution is small, the probability of interaction between the radical and pollutant molecule is also small, and under these circumstances it is very likely that the $^{\bullet}OH$ radicals would recombine $\left(2^{\bullet}OH \leftrightarrow H_2O_2\right)$ to give H_2O_2, which is a loss of oxidation potential. However, with Fe^{2+} being present in the medium, $^{\bullet}OH$ radicals can get regenerated from the H_2O_2 (formed due to recombination) through Fenton reactions. Any mechanical agitation applied to the medium can enhance the probability of radical-pollutant interaction, which in turn results in enhancement of degradation/decolorization. Ultrasound and cavitation also generate intense micromixing in the medium through different mechanisms such as microturbulence due to cavitation bubbles and microstreaming (i.e., oscillatory velocity of fluid elements due to ultrasound propagation).[21] This micromixing can increase the probability of interaction of radical and pollutant molecules, resulting in better utilization of the radicals (generated from either Fenton process or from the cavitation bubbles) for purpose of decolorization. If, however, H_2O_2 added externally to the medium (as one of the Fenton reagents) is in excess, it would evaporate into the cavitation bubble generating additional $^{\bullet}OH$ radicals, which could enhance the extent of decolorization. The extent of production of radicals through cavitation bubbles depends on three factors[25] (1) the bubble population in the medium, (2) extent of evaporation of H_2O_2, which in turn depends on the concentration of H_2O_2 in the solution and its partial pressure, and (3) peak temperature and pressure reached in the bubble at transient collapse, which in turn depends on frequency and pressure amplitude of the ultrasound wave. It should be noted that excess concentration of H_2O_2 in the medium could have adverse effect on degradation/decolorization as the $^{\bullet}OH$ radicals generated by either cavitation bubbles or Fenton reactions can get converted to molecular species due to scavenging action of H_2O_2 through following reactions[26]

$$^{\bullet}OH + H_2O_2 \rightarrow H_2O + HO_2^{\bullet}$$
$$^{\bullet}OH + HO_2^{\bullet} \rightarrow O_2 + H_2O$$

The dissolved oxygen in the medium also plays a critical role in the decolorization process due to the conservation of radicals, as has been demonstrated in our earlier works.[27,28] The dissolved oxygen can help conservation of the $^{\bullet}OH$ radicals generated through Fenton reactions as well as cavitation bubbles through following reaction

$$^{\bullet}OH + O_2 \leftrightarrow O^{\bullet} + HO_2^{\bullet}$$

The physical mechanism of synergy between sonolysis and Fenton reactions can be deduced by discriminating between the physical and chemical effects of ultrasound and cavitation, each of which has distinct beneficial influence on the Fenton process. The question that we try to answer is that what is the individual contribution of these effects, and which of these effects is more beneficial for the hybrid process of sono-Fenton. Moreover, we also try to identify the role played by secondary factors such as concentration of H_2O_2 in the medium and extent of dissolved oxygen content in the medium. As stated previously, we have adopted an approach of coupling experimental results with simulations of bubble dynamics for this purpose.

Materials, Methods and Simulations

This study aimed at elucidating the physical mechanism of the sono-Fenton process, i.e., identifying the interconnections between cavitation physics and Fenton chemistry. The textile dyes used in this work are only model or representative pollutants. The degradation of these dyes with sono-Fenton process has been previously reported in literature with identification of the degradation intermediates.[2] In view of

this, we have not included identification of degradation intermediates (with proposition of the degradation mechanism) in the experimental scope of this study. Experiments have been designed so as to vary the characteristics of cavitation phenomenon in the medium. The decolorization of original dye solution has been used as yardstick for illuminating the physical mechanism and synergy of the sono-Fenton process.

Materials

Following chemicals have been used in this study: ARB dye, BLH dye, ferrous sulfate heptahydrate ($FeSO_4{\cdot}7H_2O$), hydrogen peroxide (30% v/v), sulfuric acid (97%), sodium hydroxide (pellets). All the chemicals were purchased from Merck and used as received without any further pretreatment. For all experiments, Milli-Q water from Milli-Q Synthesis unit (Millipore®, USA) was used as the liquid medium.

Experimental setup

A schematic of the experimental setup is given online in the supplementary material. Sonication experiments were carried out in a conical flask (250 mL) made of borosilicate glass. Experiments were carried out with either mechanical stirring of the solution or sonication. For mechanical stirring, a magnetic stirrer (Remi Equipments, Model: LZMS3969) was used. An ultrasound bath (Jeotech, Model: UC-10, Capacity: 10 L) with frequency of 40 kHz and power of 200 W was used for sonication the medium. The bath was filled with 10 L of water as the sonication medium. This water was replaced with fresh water in every 10 min to maintain bulk liquid medium at constant temperature during the experiment. The average temperature of the bath, and, hence, the reaction solution inside the flask, varied by less than 3°C due to this procedure. Prior to the experiments, the sonication bath was characterized with calorimetric measurements for actual power dissipation and the distribution of acoustic pressure amplitude.[25,29] The ultrasound intensity (and, hence, the ultrasound pressure amplitude) in the bath shows significant spatial variation. To avoid the variation in the ultrasound pressure amplitude in different experiments (which could give rise to artifacts), the conical flask containing dye solution was placed at the center of the sonication bath, and its position was carefully maintained constant in all experiments. All sonication experiments were conducted in the same flask so as to have same ultrasound pressure amplitude and power dissipation in the reaction mixture in all experiments. Moreover, sonication experiments were carried out at two static pressures, viz. atmospheric (101.3 kPa) static pressure and elevated static pressure of 200 kPa (or 2 bar). The rationale underlying raised static pressure to the system during sonication has been described in an earlier article,[30] and will also be explained in this article subsequently. A simple procedure was used to raise the static pressure of the medium. The neck of the conical flask used in the experiments was closed using a rubber stopper with metal tube pierced in it. The outer end of the metal tube was connected to a nitrogen cylinder through two-stage pressure regulator. The pressure of the outlet gas from cylinder, and, hence, the static pressure on the dye solution could be controlled through this regulator.

Experimental procedure

A 100 ppm stock solution of the dye (both ARB and BLH) was prepared and stored at 4°C. The major experimental parameters that influence the decolorization process are (1) composition of the Fenton reagent (i.e., the ratio of Fe^{2+}/H_2O_2), (2) the initial concentration of dye, and (3) pH of the solution. To assess the optimum values of these parameters, we conducted preliminary experiments with ARB dye, which have been described online in the supplementary material.

For all experiments, 50 mL of dye solution of concentration 10 ppm was prepared by taking an appropriate amount of stock solution and diluting it with Milli-Q water. The experiments were carried out in seven categories for both dyes with different conditions, as described in Table 2. Prior to the main set of experiments, we conducted several preliminary experiments in which the influence of parameters such as initial dye concentration, ratio of Fenton reagents (i.e., H_2O_2 and $FeSO_4 \cdot 7H_2O$) and pH of the solution was assessed. The optimum value of each parameter was decided on the basis of these preliminary experiments (see supplementary material for greater details) and was further used for the main set of experiments. To monitor the progress of decolorization of dye solution, aliquots of 1 mL were withdrawn from the reaction mixture every 10 min, and the total time of treatment of dye solution in each category of experiments was 60 min. During the withdrawal of the aliquot, the pressure in the conical flask was released. The pressure was restored prior to commencement of sonication. After withdrawal of aliquot, the Fenton reaction was terminated by adjusting the pH 7.5– 8.0 with NaOH stock solution (5 N), which also resulted in Fe(III) floc formation. The samples were then filtered through 0.22 μm filter to remove the Fe(III) floc and the filtrate was analyzed for the concentration of dye using UV–visible spectrophotometer (Varian Carry 50). The maximum absorbance wavelength (λ_{max}) of ARB and BLH were determined at 512 nm and 586 nm, respectively, by scanning the UV–vis spectra from 200 to 800 nm. Figures 1A and B depict the UV-vis spectra of samples of the dye solutions withdrawn from the reaction mixtures at different time intervals. The decolorization efficiency in different experimental categories was determined as $\eta\,(\%) = (C_o - C)/C_o \times 100$, where, C_o is the initial concentration of dye, and C is the concentration of dye at any time t (min). In each of the seven categories of experiments for both dyes, experimental runs were taken in triplicate to check the reproducibility of the results. The mean value of the three experimental runs was used for evaluation of kinetics of decolorization and the final yield.

Bubble Dynamics Model

Cavitation is essentially the nucleation, growth and implosive collapse of gas bubbles (or more generally, the radial motion or volume oscillations of the bubble) driven by bulk pressure variation induced by ultrasound. Depending on the pressure amplitude of the ultrasound wave and static pressure in the medium, the radial motion of the bubble is characterized as stable cavitation and transient cavitation. The transient collapse of the bubble is extremely fast and adiabatic during which the bubble wall velocity reaches (or even exceeds) the sonic speed in the liquid medium. The bubble can get compressed to an extremely small size (typically 1/10th to 1/100th of original size), and temperature and pressure in it can reach to extreme (~5000 K, ~500 bar). This essentially creates energy concentration in the medium on extremely small spatial and temporal scale, as the bubble

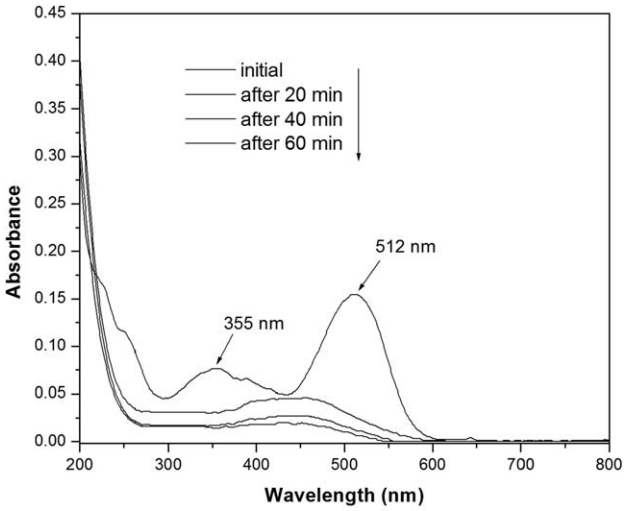

(A)

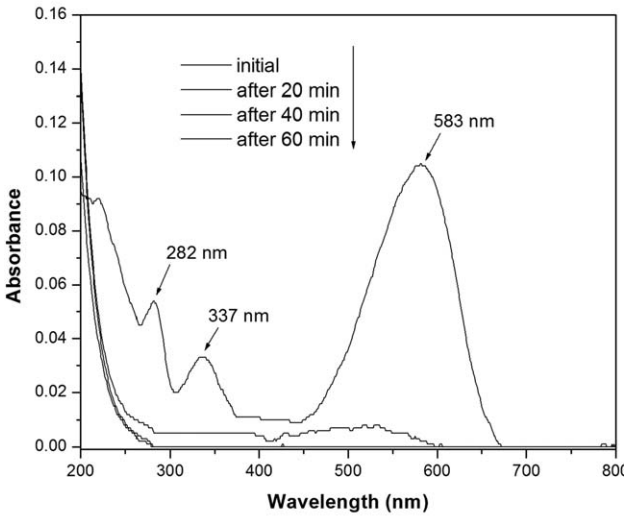

(B)

Figure 1. (A) UV–visible spectra of ARB for different samples withdrawn at different time interval during Fenton reaction, and (B) UV–visible spectra of BLH for different samples withdrawn at different time interval during Fenton reaction.

collapse occurs in a few tens of nanoseconds. During the transient collapse, the bubble contents (which is a mixture of gas and vapor of bulk liquid medium) are subjected to extreme conditions generated in the bubble and can get dissociated to form various species, some of which are radical species. The most common liquid medium used for cavitation assisted reactions is water and the species arising out of dissociation of water contain many radicals such as $H^{\bullet}$, $O^{\bullet}$ and $^{\bullet}OH$. For small bubbles of few microns size and frequencies in the range of 20–100 kHz, transient cavitation is seen for ultrasound pressure amplitudes greater than the static pressure on the medium. If the static pressure of the medium is raised to moderate levels, keeping the acoustic pressure amplitude constant, the transient cavitation events get eliminated as the static pressure exceeds the ultrasound pressure amplitude. In such cases, the bubble undergoes stable, small-amplitude oscillatory motion. The temperature and pressure inside the bubble remains almost ambient. The ultrasound wave (which is a longitudinal wave comprising of alternate compression/rarefaction cycles) also induces high-velocity oscillatory motion of the fluid elements, commonly known as microstreaming. However, the liquid properties such as density and compressibility are not a strong function of pressure, and, hence, the velocity of microstreaming is not altered by rise in the static pressure on the liquid medium.

The principal chemical effect of cavitation, popularly known as the *sonochemical effect* is generation of highly reactive radicals such as $^{\bullet}H$, $^{\bullet}O$, $^{\bullet}OH$ and $HO_2^{\bullet}$. These radicals render several beneficial effects on a reaction system such as induction of stubborn chemical reaction, acceleration of the reaction kinetics, reduction in the number of steps in a synthesis or sometimes a switch of reaction pathway. The principal physical effect of cavitation is generation of strong convection in the medium due to five phenomena, viz. ultrasound oscillatory velocity, microconvection (or microturbulence), microstreaming, shock waves and microjets. As both physical and chemical effects of cavitation occur on extremely small spatial and temporal scale, a direct measurement or quantification of these effects would require highly sophisticated equipment. However, a much easier (and cheaper) method to get a fairly accurate estimate of the magnitudes of physical and chemical effects of cavitation is numerical simulations of the bubble dynamics equation, which we rely on in this study. Modeling of cavitation bubble dynamics is an active area of research for past 3 decades and various authors have addressed the matter with different approaches. We refer the reader to our earlier article for a review of these studies.[31] We have used the diffusion limited ordinary differential equation (ODE) model using boundary layer approximation proposed by Toegel et al. for our analysis,[32] which is based on the comprehensive PDE model of Storey and Szeri,[22] who showed that vapor entrapment in the cavitation bubble, leading to formation of radicals is essentially a diffusion limited process. Large amount of evaporation occurs at the bubble interface during the expansion phase of bubble motion, and vapor molecules enter and diffuse toward the bubble core. In the subsequent compression phase, the same vapor diffuses back and condenses at the bubble wall. However, in the final moments of bubble compression, velocity of the bubble interface (or bubble wall) becomes extremely fast and the time scale of bubble motion becomes smaller than the time scale of vapor diffusion to bubble wall as well as time scale of condensation (or phase change) at the bubble wall. As a result, not all of the vapor that has entered the bubble during expansion can escape during compression. The entrapped vapor is subjected to conditions of extreme pressure and temperature reached during collapse. Dissociation of the vapor molecules occurs at these conditions resulting in generation of radicals. This model has been extensively described in our previous articles.[33,34] For the convenience of the reader, we reproduce here only the main components of the model and relevant data/boundary conditions. For greater details on this model, we refer the reader to our earlier articles[33,34] as well as the original article of Toegel et al.,[32] and Storey and Szeri.[22]

The essential equations and thermodynamic data of this model have been summarized in Tables 1a and 1b. The main components of the model are:

1. Keller-Miksis equation for the radial motion of the bubble.[35]

Table 1a. Model Equation for Cavitation Bubble Dynamics

Model Component	Equation	Initial Value
1. Radial motion of the cavitation bubble	$\left(1-\frac{dR/dt}{c}\right)R\frac{d^2R}{dt^2}+\frac{3}{2}\left(1-\frac{dR/dt}{3c}\right)\left(\frac{dR}{dt}\right)^2=\frac{1}{\rho_L}\left(1+\frac{dR/dt}{c}\right)(P_i-P_t)+\frac{R}{\rho_L c}\frac{dP_i}{dt}-4v\frac{dR/dt}{R}-\frac{2\sigma}{\rho_L R}$	At $t=0$, $R=R_o$, $dR/dt=0$
	Internal pressure in the bubble: $P_i=\frac{N_{tot}(t)\,kT}{[4\pi(R^3(t)-h^3)/3]}$	
	Pressure in bulk liquid medium: $P_t=P_0-P_A\sin(2\pi ft)$	
2. Diffusive flux of water molecules	$\frac{dN_W}{dt}=4\pi R^2 D_W\frac{\partial C_W}{\partial r}\mid_{r=R}\approx 4\pi R^2 D_W\left(\frac{C_{W,R}-C_W}{l_{diff}}\right)$	At $t=0$, $N_w=0$
	Instantaneous diffusive penetration depth: $l_{diff}=\min\left(\sqrt{\frac{RD_w}{\lvert dR/dt\rvert}},\frac{R}{\pi}\right)$	
3. Heat conduction across bubble wall	$\frac{dQ}{dt}=4\pi R^2\lambda\frac{\partial T}{\partial r}\mid_{r=R}\approx 4\pi R^2\lambda\left(\frac{T_0-T}{l_{th}}\right)$	At $t=0$, $Q=0$
	Thermal diffusion length: $l_{th}=\min\left(\sqrt{\frac{R\kappa}{\lvert dR/dt\rvert}},\frac{R}{\pi}\right)$	
4. Overall energy balance	$C_{V,mix}\,dT/dt=dQ/dt-P_i dV/dt+(h_W-U_W)dN_W/dt$	At $t=0$, $T=T_0$
	Mixture heat capacity: $C_{V,mix}=\sum C_{V,i}N_i$ $(i=N_2/O_2/H_2O)$	
	Molecular properties of water:	
	Enthalpy: $h_w=4kT_o$	
	Internal energy: $U_W=N_W kT\left(3+\sum_{i=1}^{3}\frac{\theta_i/T}{\exp(\theta_i/T)-1}\right)$	
	Heat capacity of various species $(i=N_2/O_2/H_2O)$: $C_{V,i}=N_i k\left(f_i/2+\sum\left((\theta_i/T)^2\exp(\theta_i/T)/(\exp(\theta_i/T)-1)^2\right)\right)$	

Terms and definitions for Table 1a: R is the radius of the bubble, dR/dt is the bubble wall velocity, c is the velocity of sound in bulk liquid medium, ρ_L is the density of the liquid, v is the kinematic viscosity of liquid, σ is the surface tension of liquid, λ is the thermal conductivity of bubble contents, κ is the thermal diffusivity of bubble contents, θ is the characteristic vibrational temperature(s) of the species, N_w is the number of water molecules in the bubble, N_{N2} is the number of nitrogen molecules in the bubble, N_{O2} is the number of oxygen molecules in the bubble, t is the time, D_w is the diffusion coefficient of water vapor, C_w is the concentration of water molecules in the bubble, $C_{w,R}$ is the concentration of water molecules at the bubble wall or gas-liquid interface, Q is the heat conducted across bubble wall, T is the temperature of the bubble contents, T_o is the ambient (or bulk liquid medium) temperature, k is the Bolzmann constant, h_w is the molecular enthalpy of water, U_w is the internal energy of water molecules, f_i is the translational and rotational degrees of freedom; $C_{V,i}$ is the heat capacity at constant volume for species I, N_{tot} is the total number of molecules (gas + vapor) in the bubble, h is the van der Waal's hard core radius, P_o is the ambient (bulk) pressure in liquid, P_A is the pressure amplitude of ultrasound wave, and f is the frequency of ultrasound wave.

Table 1b. Thermodynamic Data for the Model

Species	Degrees of freedom (translational + rotational) (f_i)	Lennard–Jones force constants		Characteristic vibrational temperatures θ (K)
		σ (10^{-10} m)	ε/k (K)	
N_2	5	3.68	92	3350
O_2	5	3.43	113	2273
H_2O	6	2.65	380	2295, 5255, 5400

Data taken from Hirschfelder et al.[41] Condon and Odishaw,[42] Reid et al.[43]

2. Equation for the diffusive flux of water vapor and heat conduction through bubble wall.
3. Overall energy balance treating the cavitation bubble as an open system.

The transport parameters for the heat and mass transfer (thermal conductivity and diffusion coefficient) are determined using Chapman-Enskog theory using Lennard-Jones 12-6 potential at the bulk temperature of the liquid medium. Thermal and diffusive penetration depths are estimated using dimensional analysis. Diffusion of gas across bubble interface is ignored in this model as the time scale for the diffusion of gases is much higher than the time scale for the radial motion of bubble. The set of four ODEs described in Table 1a was solved simultaneously using Runge-Kutta adaptive step-size method.[36] We have considered an air bubble (for aerated solutions) and a nitrogen bubble (for deaerated solution using nitrogen sparging) as the cavitation nuclei for simulations of cavitation bubble dynamics in the dye solution. The condition for bubble collapse is taken as the first compression after an initial expansion. Various parameters used in the simulation of bubble dynamics equation and their numerical values are as follows: Ultrasound frequency (f) = 40 kHz; ultrasound pressure amplitude (P_A) = 200 kPa; equilibrium bubble radius (R_o) = 5 μm; vapor pressure of liquid medium (water) = 2,500 Pa (calculated using Antoine type correlation). Various physical properties of water are as follows: density (ρ_L) = 1000 kg/m^3, kinematic viscosity (v) = 10^{-6} Pa-s, surface tension (σ) = 0.072 N/m and velocity of sound (c) = 1481 m/s. Since the dyes as well as other components of reaction mixture (H_2O_2, $FeSO_4 \cdot 7H_2O$) are present in very small quantities, we have ignored the change in the physical properties of water with addition of these chemicals.

Estimation of physical and chemical effects of cavitation

Sonochemical Effect (radical generation by cavitation bubbles): Using the numerical solution of bubble dynamics model, one can estimate the composition of the bubble contents at the collapse. Although calculating the composition of the bubble at the time of collapse, we assume that thermodynamic equilibrium is attained.[31] The equilibrium mole fraction of the various species in the bubble at the conditions of temperature and pressure at first the compression of the

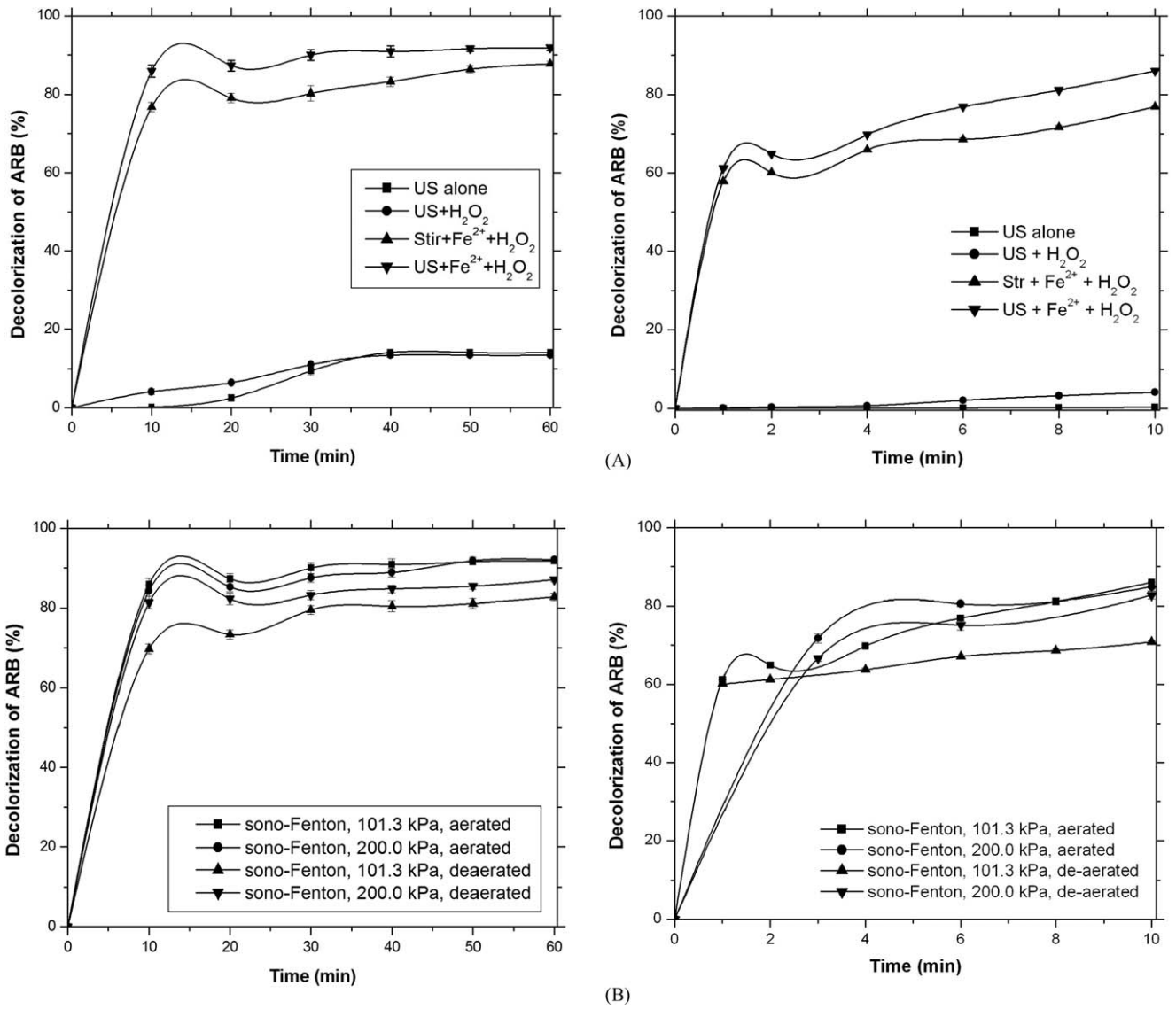

Figure 2. Experimental results for decolorization of ARB dye solution (10 ppm).

(A) Decolorization under different combinations of ultrasound and Fenton reagents at atmospheric static pressure (A.1 is the time history of total 60 min reaction, A.2 are the trends of decolorization in the initial 10 min), and (B) effect of static pressure on decolorization by sono-Fenton process (B.1 is the time history of total 60 min reaction, B.2 are trends of decolorization in the initial 10 min).

bubble can be calculated using free-energy minimization technique.[37]

Sonophysical Effect of Cavitation: The principal physical effect of cavitation is generation of convection in the bulk medium through two phenomena, viz. microconvection, shock or acoustic waves. These two parameters can be calculated from numerical result of bubble dynamics model as follows[38–40]

Microconvection: $V_{\text{turb}}(r,t) = \frac{R^2}{r^2}\left(\frac{dR}{dt}\right)$

Shock Waves (or acoustic waves): $P_{AW}(r,t) = \frac{\rho}{4\pi r}\frac{d^2V_b}{dt^2} = \rho\frac{R}{r}\left[2\left(\frac{dR}{dt}\right)^2 + R\frac{d^2R}{dt^2}\right]$

where V_b is the volume of the bubble. A representative value of r is taken as 1 mm. Simulations have been conducted for the following four conditions (1) air bubble, atmospheric static pressure, (2) air bubble, elevated static pressure, (3) nitrogen bubble, atmospheric static pressure, and (4) Nitrogen bubble, elevated static pressure.

Results and Discussion

Experimental results

The time history of decolorization of ARB and BLH dyes during 60 min of reaction is shown in Figures 2 and 3, respectively. The decolorization reaction is very fast and it could be seen from Figures 2 and 3 that for both dyes, most of the decolorization was achieved in the first 10 min of treatment in the categories involving Fenton reagent. Therefore, in Figures 2 and 3, we have separately depicted the trends in decolorization of both dyes for the first 10 min in Figures 2A.2, 2B.2, 3A.2, and 3B.2, with analysis of samples that were withdrawn every 2 min. The summary of the decolorization experiments is given in Table 2, which gives the extent of decolorization at the end of 10 min as well as 60 min. The time history of decolorization in the first 10 min was fitted to pseudo first-order kinetics to determine the kinetic constant of decolorization. We would like to state

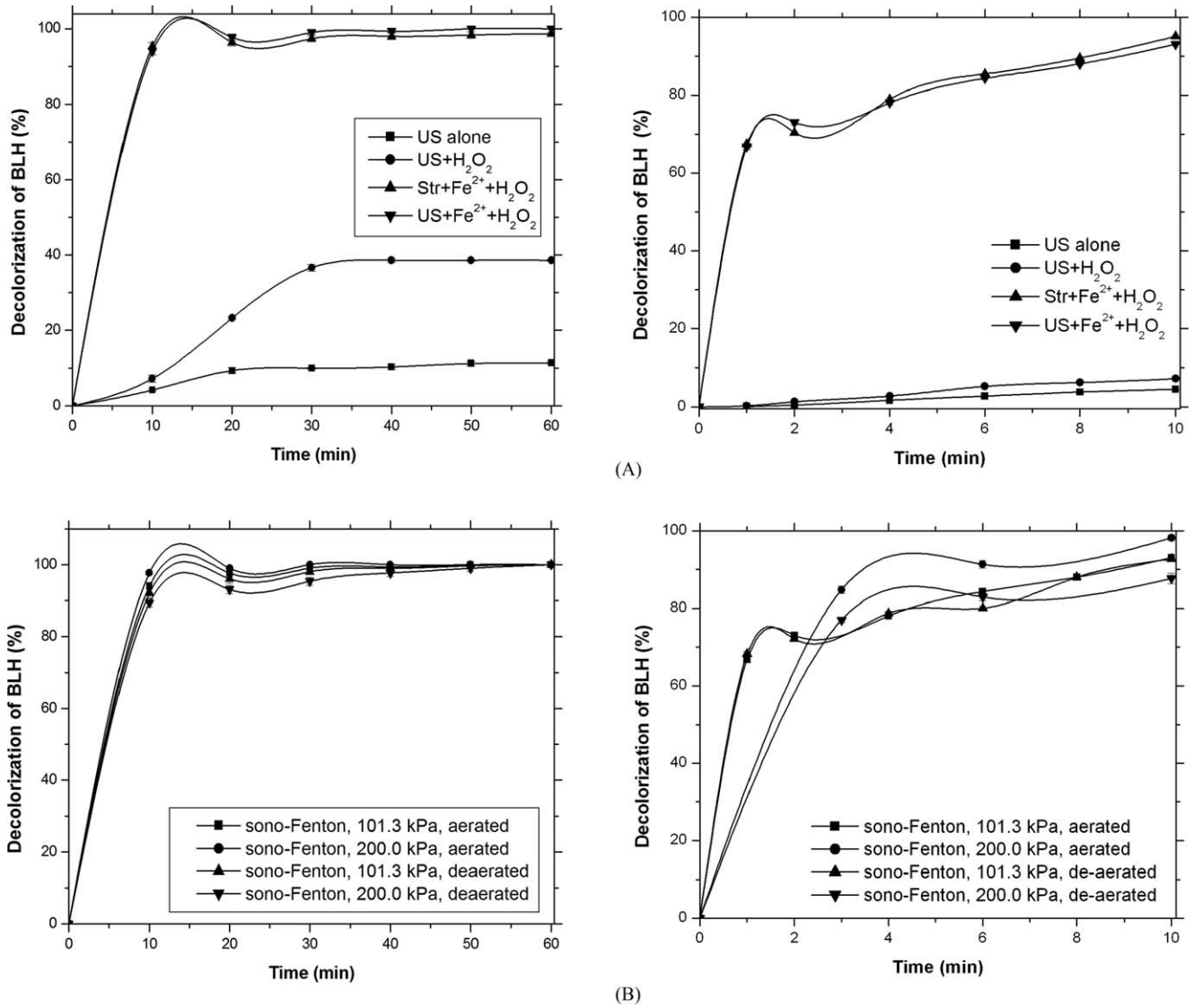

Figure 3. Experimental results for decolorization of BLH dye solution (10 ppm).

(A) Decolorization under different combinations of ultrasound and Fenton reagents at atmospheric static pressure (A.1 is the time history of total 60 min reaction, A.2 are trends of decolorization in the initial 10 min), and (B) effect of static pressure on decolorization by sono-Fenton process (B.1 is the time history of total 60 min reaction, B.2 are trends of decolorization in the initial 10 min).

that we have not explicitly determined the order of the decolorization reaction. The decolorization process (which essentially is the oxidation of the dye molecules induced by radicals produced during sonication and Fenton reaction) occurs through series of reactions with several intermediates. Each of the reaction in decolorization chain will have its own order and rate constant. In view of this difficulty, and the limitations of instrumentation used in the study, we have made a simple approximation of first-order overall reaction behavior, to get a relative idea of the kinetics of decolorization under different experimental conditions. Since most of the decolorization in experiments employing Fenton reagent occurred within first 10 min, the first-order kinetic constant for these experiments was calculated only with the decolorization data for 10 min. The fitness of the pseudo first-order kinetic model to the experimental data is represented by the regression coefficient (R^2), which is also mentioned in Table 2. For most cases, the value of R^2 was greater than 0.8, which indicates suitability of the pseudo first-order kinetics for the time data of decolorization.

For categories involving only sonication or sonication with H_2O_2, the rate of degradation/decolorization was linear up to 30 min of treatment, and leveled off thereafter, with no further decolorization. Some other observations are as follows:

- Comparing between the two dyes in all categories of experiments, we see higher decolorization for the BLH dye, which is a nonazo category dye.
- The total decolorization obtained for both dyes for categories involving Fenton reagents was significantly higher than the categories where either sonication alone or sonication with H_2O_2 was applied.
- The decolorization kinetics as well as total decolorization obtained with Fenton reagent coupled with either mechanical stirring or ultrasound was similar.

Table 2. Summary of Experimental Results

Experimental categories and conditions/composition of reaction mixture in each category	ARB dye (10 ppm)			BLH dye (10 ppm)		
	η (%)[a]		k_1	η (%)[a]		k_1
	10 min	60 min	(min^{-1})	10 min	60 min	(min^{-1})
(1) Sonication alone (50 mL dye solution of concn.10 ppm, P_o = 101.3 kPa)	0.20 ± 0.14	14.04 ± 0.04	0.0003 (R^2 = 0.96)	4.24 ± 0.38	11.43 ± 0.38	0.0047 (R^2 = 0.98)
(2) Stirring + Fenton (50 mL dye solution of concn. 10 ppm + 2.5 mg $FeSO_4 \cdot 7H_2O$ + 27 μL 30% H_2O_2, P_o = 101.3 kPa)	76.81 ± 1.20	87.72 ± 0.68	0.2 (R^2 = 0.65)	95.38 ± 0.99	98.68 ± 0.38	0.33 (R^2 = 0.87)
(3) Sonication + H_2O_2 (50 mL dye solution of 10 ppm concn. + 27 μL 30% H_2O_2, P_o = 101.3 kPa)	4.12 ± 0.70	13.35 ± 0.37	0.004 (R^2 = 0.91)	7.24 ± 0.94	38.59 ± 0.29	0.0079 (R^2 = 0.98)
(4) Sonication + Fenton (50 mL dye solution of 10 ppm concn. + 2.5 mg $FeSO_4 \cdot 7H_2O$ + 27 μL 30% H_2O_2, P_o = 101.3 kPa)	85.9 ± 1.55	91.81 ± 0.73	0.25 (R^2 = 0.77)	94.06 ± 0.91	100.0 ± 0	0.31 (R^2 = 0.81)
(5) Sonication + Fenton (50 mL dye solution of 10 ppm concn. + 2.5 mg $FeSO_4 \cdot 7H_2O$ + 27 μL 30% H_2O_2, P_o = 200 kPa)	84.31 ± 1.43	92.04 ± 0.53	0.24 (R^2 = 0.81)	97.69 ± 0.58	100.0 ± 0	0.42 (R^2 = 0.96)
(6) Sonication + Fenton (deaerated solution#, 50 mL dye solution of 10 ppm concn. + 2.5 mg $FeSO_4 \cdot 7H_2O$ + 27 μL 30% H_2O_2, P_o = 101.3 kPa)	69.76 ± 1.21	82.72 ± 0.93	0.2 (R^2 = 0.51)	92.08 ± 1.3	100.0 ± 0	0.31 (R^2 = 0.8)
(7) Sonication + Fenton (deaerated solution#, 50 mL dye solution of 10 ppm concn. + 2.5 mg $FeSO_4 \cdot 7H_2O$ + 27 μL 30% H_2O_2, P_o = 200 kPa)	81.35 ± 1.52	87.04 ± 0.53	0.21 (R^2 = 0.85)	89.44 ± 1.07	100.0 ± 0	0.27 (R^2 = 0.79)

[a]Initial pH of dye solution in all experiments was 2.0. The decolorization efficiency (η in %, as defined in subsection *Experimental procedure*), and the kinetic constant for each experimental category refers to the mean value ± standard deviation of the three experimental runs in that category.
Deaeration to 2 ppm of dissolved oxygen achieved using sparging the dye solution with nitrogen at flow rate of 40 lit/h, P_o is the static pressure on the medium, k_1 is the pseudo first-order kinetic constant calculated on the basis of decolorization obtained in the first 10 min of the reaction, and R^2 is the regression coefficient.

- In case of sonication experiments, addition of H_2O_2 to the dye solution alone does not seem to cause any major change in extent of decolorization of the ARB dye, although a marginal enhancement in decolorization of the BLH dye is seen.
- For the sono-Fenton process in aerated dye solution (i.e., category 4 and 5 of experiments), the extent of decolorization for both dyes is same for both atmospheric as well as elevated static pressure. Quite interestingly, in experimental categories 6 and 7, the extent of decolorization by the sono-Fenton process (at both atmospheric and elevated static pressure) reduces marginally with deaeration (or essentially deoxygenation) of the medium for the ARB dye. On the other hand, the decolorization of the BLH dye remains unaffected by the deaeration of the medium.

Simulations results

As stated earlier, the simulations were carried out for four conditions for air and nitrogen bubble. Representative simulations results for air bubble at atmospheric static pressure are shown in Figure 4, while all results have been depicted in the supplementary material provided with the manuscript. The summary of the simulations results is given in Table 3a that lists the peak conditions of temperature and pressure reached in the bubble at moment transient collapse, the magnitudes of the microconvection velocity and the acoustic wave generated by the cavitation bubble, and the equilibrium composition of chemical species generated from dissociation of gas and water vapor inside the bubble at the moment of transient collapse. From these results, we can identify some peculiar features of the cavitation bubble dynamics at the conditions used in the experiments.

1. Both air and nitrogen bubbles undergo intense collapse at atmospheric static pressure. The peak conditions reached in the nitrogen bubble are more intense than air bubble. The velocity of microconvection generated by both bubbles is similar, but the acoustic waves emitted by nitrogen bubble are stronger than those by the air bubble. The extent of water vapor entrapment in nitrogen bubble is higher than air bubble.
2. Quite interestingly, although the peak conditions of temperature and pressure reached during transient collapse of air bubbles are lower than nitrogen bubble, the radical production by air bubble is higher. The number of oxidizing radicals ($^{\bullet}O$, $HO_2^{\bullet}$ and $^{\bullet}OH$) produced by the air bubble at least two fold higher. We attribute this result to the presence of oxygen in air bubble that conserves the radicals formed out of dissociation of water vapor.[27,28]
3. With rise in static pressure to 200 kPa (or 2 bar), both chemical and physical effects of cavitation bubbles get eliminated. The radical production in both bubbles becomes practically nil, and the magnitudes of the microconvection velocity and pressure amplitude of the acoustic wave reduces drastically. This essentially means that the contribution of transient cavitation to the overall decolorization process is eliminated with rise in static pressure. Application of high-static pressure in the medium (greater or equal to the acoustic pressure amplitude) can help in segregation of the effects of ultrasound and transient cavitation in the medium.

Analysis and discernment of the synergy in sono-Fenton process

Analysis of the experimental and simulation results concurrently helps us to discern the mechanism of the hybrid sono-Fenton process, and also identify the links between individual (and seeming independent) mechanism of sonochemical and Fenton processes. Comparison of results of categories 1 and 2, where the two techniques were applied separately, shows that contribution of Fenton process to overall decolorization is much higher than sonolysis. Comparison of decolorization obtained in categories 2 and 4 indicates a very small rise in decolorization with sono-Fenton

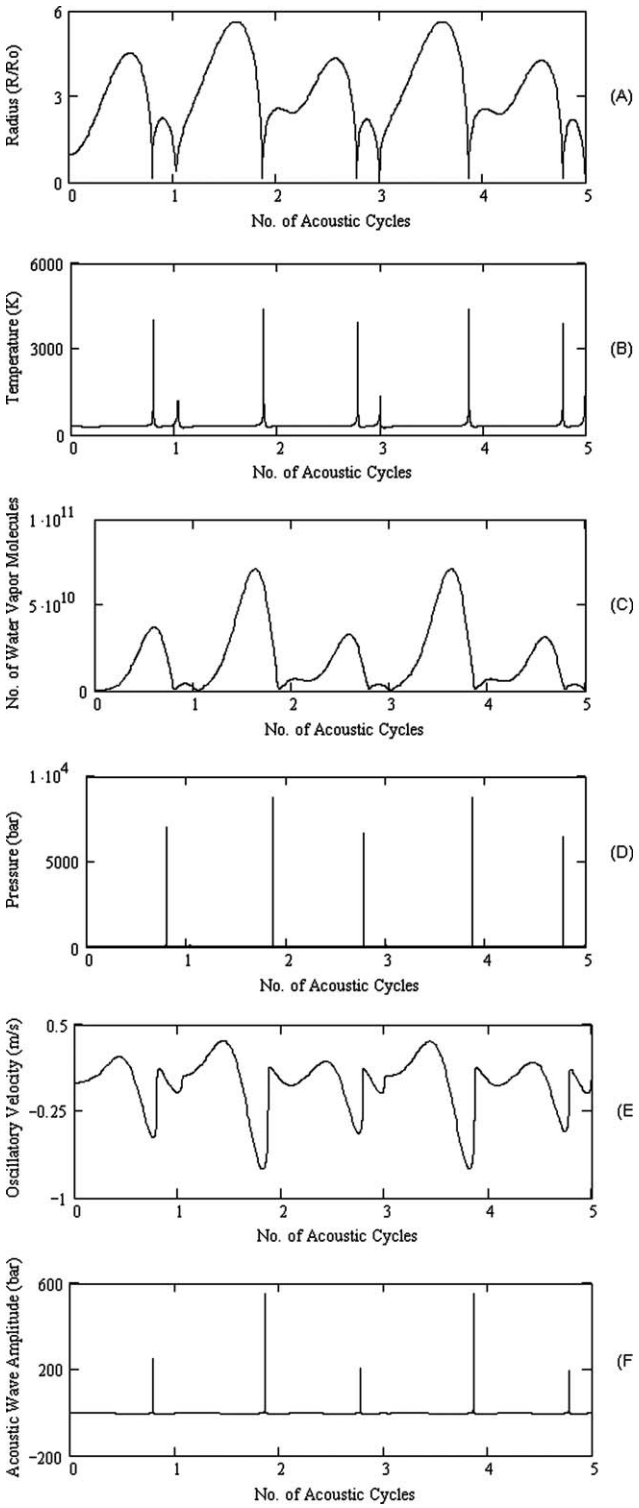

Figure 4. Simulations of radial motion of a 5 μm air bubble in water.

(*f*: 40 kHz; P_A: 200 kPa; P_o: 101.3 kPa (atmospheric). Time history of (A) radius of the bubble, (B) temperature inside the bubble, (C) water vapor evaporation in the bubble, (D) pressure inside the bubble, (E) microturbulence generated by the bubble, and (F) acoustic waves emitted by the bubble.

process, as compared to Fenton process alone. Practically same decolorization as in category 4 is obtained in category 5, in which the contribution of transient cavitation effect is eliminated at elevated static pressure. These results are clearly indicative of the dominant role played by Fenton process over the sonochemical process. The most probable cause leading to this effect is scavenging of the $^{\bullet}OH$ radicals generated by the cavitation bubbles by the H_2O_2 through following reactions,[26] which leads to formation of molecular species causing reduction in the oxidation or decolorization potential

$$^{\bullet}OH + H_2O_2 \rightarrow H_2O + HO_2^{\bullet}$$

$$H^{\bullet} + H_2O_2 \rightarrow HO_2^{\bullet} + H_2$$

$$HO_2^{\bullet} + {}^{\bullet}OH \rightarrow O_2 + H_2O$$

The synergy in sonochemical and Fenton process thus seems to be negative.

Another factor leading to smaller contribution of sonolysis in the sono-Fenton process is the discrete nature of production of $^{\bullet}OH$ radicals by cavitation bubbles. The population or number density of cavitation bubbles in the medium is not likely to be uniform volumetrically, and so is the production of $^{\bullet}OH$ radicals through transient cavitation events. The concentration of dye molecules in the solution is relatively small (10 ppm), and, hence, the probability of dye-radical interaction also comes into picture. Discrete production of $^{\bullet}OH$ in the reaction volume, together with low concentration of dye can lead to lower utilization of the radicals produced by transient cavitation events for decolorization. The dissolved oxygen in the medium is revealed to play major role. The oxygen can conserve $^{\bullet}OH$ radicals to generate other oxidizing species like $^{\bullet}O$ and $^{\bullet}OH_2$ through reaction[26]

$$^{\bullet}OH + O_2 \rightarrow HO_2^{\bullet} + O^{\bullet}$$

At lower concentration of dissolved oxygen (with deaeration of the medium), as in experimental categories 6 and 7, the conservation action is reduced, which eventually results in loss of radicals resulting in lower decolorization.

Conclusion

In this study, we have attempted to discern the mechanism of the hybrid sono-Fenton process for decolorization of the textile dyes. The concurrent analysis of experimental results with the simulations of cavitation bubble dynamics reveals the links and interactions between the individual mechanism of sonolysis and Fenton process. H_2O_2 added to the medium as one of the Fenton reagent scavenges the $^{\bullet}OH$ radicals produced by cavitation bubbles, which nullify their effect, giving a negative synergy between sonolysis and Fenton process. Mere addition of H_2O_2 to the medium during sonolysis does not give much enhancement to decolorization, which is attributed to lower vapor pressure of H_2O_2 due to which it does not evaporate and dissociate inside the bubble (to generate additional $^{\bullet}OH$ radicals). Fenton reagent ($Fe^{2+} + H_2O_2$), on the other hand, gives volumetrically more uniform production of $^{\bullet}OH$ radicals in the solution, and, hence, has a dominating contribution to decolorization in the hybrid process. The role of ultrasound and cavitation in the hybrid sono-Fenton process is simply physical, i.e., causing intense mixing in the medium. Radical conservation due to dissolved oxygen is also revealed to play a major role in effective utilization of $^{\bullet}OH$ radicals for decolorization.

Table 3a. Summary of the Simulation Results (Air and N_2 Bubbles)

Species	Parameters for simulations			
	Air bubble $R_o = 5\ \mu m$ $P_o = 101.3$ kPa	Air bubble $R_o = 5\ \mu m$ $P_o = 200$ kPa	Nitrogen bubble $R_o = 5\ \mu m$ $P_o = 101.3$ kPa	Nitrogen bubble $R_o = 5\ \mu m$ $P_o = 200$ kPa
	Conditions at the first collapse of the bubble			
	$T_{max} = 4013$ K $P_{max} = 705.6$ MPa $V_{turb} = 0.056$ m/s $P_{AW} = 2.53$ MPa $N_{N2} = 1.306E+10$ $N_{O2} = 3.471E+9$ $N_W = 2.026E+9$	$T_{max} = 1075$ K $P_{max} = 7.78$ MPa $V_{turb} = 0.008$ m/s $P_{AW} = 0.22$ MPa $N_{N2} = 1.306E+10$ $N_{O2} = 3.471E+9$ $N_W = 9.03E+8$	$T_{max} = 4345$ K $P_{max} = 786.6$ MPa $V_{turb} = 0.054$ m/s $P_{AW} = 5.89$ MPa $N_{N2} = 1.653E+10$ $N_W = 2.872E+9$	$T_{max} = 1106$ K $P_{max} = 15$ MPa $V_{turb} = 0.008$ m/s $P_{AW} = 0.3$ MPa $N_{N2} = 1.653E+10$ $N_W = 1.28E+9$
	Equilibrium composition of species in the bubble at collapse			
N_2	6.52E–01	7.49E–01	8.26E–01	9.28E–01
O_2	1.30E–01	1.99E–01	2.29E–03	0.
H_2O	9.21E–02	5.20E–02	1.08E–01	7.20E–02
H	8.15E–04	0.	5.08E–03	0.
O	6.50E–03	0.	1.47E–03	0.
OH	2.56E–02	1.12E–07	1.42E–02	0.
HO_2	1.11E–03	0.	8.12E–05	0.
H_2O_2	1.69E–04	0.	3.65E–05	0.
O_3	1.67E–05	0.	5.75E–08	0.
H_2	1.79E–03	0.	2.68E–02	6.74E–08
NO	8.79E–02	7.13E–05	1.61E–02	3.11E–08
NO_2	1.67E–03	1.98E–05	3.76E–05	0.
HNO	1.55E–04	0.	1.18E–04	0.
HNO_2	1.16E–05	0.	8.73E–07	0.
HNO_3	1.58E–06	0.	1.48E–08	0.
NH_3	1.89E–06	0.	1.24E–04	0.

Terms and definitions for Table 3a: P_o is the static pressure in the liquid medium, R_o is initial radius of the cavitation bubble, V_{turb} is the average velocity of the microturbulence in the medium generated by ultrasound and cavitation in the medium (estimated at 1 mm distance from bubble center), P_{AW} is the pressure amplitude of the acoustic wave generated by the cavitation bubble, T_{max} is the temperature peak reached in the bubble at the time of first collapse, P_{max} is the pressure peak reached in the bubble at the time of first collapse, N_W is the number of water molecules trapped in the bubble, N_{N2} is the number of N_2 molecules in the bubble, N_{O2} is the number of oxygen molecules in the bubble, N_{OH} is the number of OH radicals present in the bubble at transient collapse, N_H is the number of H radicals present in the bubble at transient collapse, N_O is the number of O radicals present in the bubble at transient collapse, N_{HO2} is the number of HO_2 radicals present in the bubble at transient collapse, and N_{H2O2} is the number of H_2O_2 molecules present in the bubble at transient collapse.

Table 3b. Net Production of Various Oxidizing Species per Bubble

Parameter	Air bubble ($P_o = 101.3$ kPa)	Air bubble ($P_o = 200$ kPa)	N_2 bubble ($P_o = 101.3$ kPa)	N_2 bubble ($P_o = 200$ kPa)
N_{OH}	4.75E+8	1.95E+3	2.75E+8	0.
N_O	1.2E+8	0.	2.85E+7	0.
N_{HO2}	2.06E+7	0.	1.58E+6	0.
N_{H2O2}	3.14E+6	0.	7.08E+5	0.

Acknowledgments

The authors are grateful to the anonymous referees of this article for their meticulous assessment of this manuscript and constructive criticism.

Literature Cited

1. Peralta-Zamora P, Kunz A, de Moraes SG, Pelegrini R, de Campos Moleiro P, Reyes J, Duran N. Degradation of reactive dyes I. A comparative study of ozonation, enzymatic and photochemical processes. *Chemosphere*. 1998;38:835–852.
2. Lin JJ, Zhao XS, Liu D, Yu ZG, Zhang Y, Xu H. The decoloration and mineralization of azo dye C.I. Acid Red 14 by sonochemical process: Rate improvement via Fenton's reactions. *J Hazard Mater*. 2008;157:541–546.
3. Wu CH. Decolorization of C.I. reactive red 2 in O3, Fenton-like and O3/Fenton-like hybrid systems. *Dyes Pigm*. 2008;77:24–30.
4. Papić S, Vujević D, Koprivanac N, Šinko D. Decolorization and mineralization of commercial reactive dyes by using homogeneous and heterogeneous Fenton and UV/Fenton process. *J Hazard Mater*. 2009;164:1137–1145.
5. Patidar R, Khanna S, Moholkar VS. Physical features of ultrasound assisted enzymatic degradation of recalcitrant organic pollutants. *Ultrason Sonochem*. 2012;19:104–118.
6. Gogate PR, Pandit AB. A review of imperative technologies for wastewater treatment I: oxidation technologies at ambient conditions. *Adv Environ Res*. 2004;8:501–551.
7. Gogate PR, Pandit AB. A review of imperative technologies for wastewater treatment II: hybrid methods. *Adv Environ Res*. 2004;8:553–597.
8. Segura Y, Molina R, Martinez F, Melero JA. Integrated heterogeneous sono-photo Fenton processes for the degradation of phenolic aqueous solutions. *Ultrason Sonochem*. 2008;16:417–424.
9. Segura Y, Martinez F, Melero JA, Molina R, Chand R, Bremner DH. Enhancement of the advanced Fenton process (Fe0/H2O2) by ultrasound for the mineralization of phenol. *Appl Catal B Environ*. 2012;113-114:100–106.
10. Huang R, Fang Z, Yan X, Cheng W. Heterogeneous sono-Fenton catalytic degradation of bisphenol A by Fe3O4 magnetic nanoparticles under neutral condition. *Chem Eng J*. 2012;197:242–249.
11. Babuponnusami A, Muthukumar K. Advanced oxidation of phenol: A comparison between Fenton, electro-Fenton, sono-electro-Fenton and photo-electro-Fenton processes. *Chem Eng J*. 2012;183:1–9.
12. Grčić I, Šipić A, Koprivanac N, Domagoj V. Global parameter of ultrasound exploitation (GPUE) in the reactors for wastewater treatment by sono-Fenton oxidation. *Ultrason Sonochem*. 2012;19:270–279.
13. Oezdemir C, Oeden MK, Sahinkaya S, Kalipci E. Color removal from synthetic textile wastewater by sono-Fenton process. *Clean: Soil Air Water*. 2011;39:60–67.
14. Ozdemir C, Oden MK, Sahinkaya S, Guclu D. The sonochemical decolorization of textile azo dye CI reactive orange 127. *Color Technol*. 2011;127:268–273.

15. Zhong X, Royer S, Zhang H, Huang Q, Xiang L, Valange S, Barrault J. Mesoporous silica iron-doped as stable and efficient heterogeneous catalyst for the degradation of C.I. Acid Orange 7 using sono-photo-Fenton process. *Sep Purif Technol*. 2011;80:163–171.
16. Sundararaman TR, Ramamurthi V, Partha N. Decolorization and COD removal of Reactive yellow 16 by Fenton oxidation and comparison of dye removal with photo Fenton and sono Fenton process. *Mod Appl Sci*. 2009;3:15–22.
17. Bremner DH, Molina R, Martínez F, Melero JA, Segura Y. Degradation of phenolic aqueous solutions by high frequency sono-Fenton systems (US-Fe2O3/SBA-15-H2O2). *Appl Catal B Environ.* 2009;90: 380–388.
18. Molina R, Martínez F, Melero JA, Bremner DH, Chakinala AG. Mineralization of phenol by a heterogeneous ultrasound/Fe-SBA-15/ H2O2 process: Multivariate study by factorial design of experiments. *Appl Catal B Environ*. 2006;66:198–207.
19. Bianchi CL, Pirola C, Ragaini V, Selli E. Mechanism and efficiency of atrazine degradation under combined oxidation processes. *Appl Catal B Environ*. 2006;64:131–138.
20. Andreozzi R, Caprio V, Insola A, Marotta R. Advanced oxidation processes (AOP) for water purification and recovery. *Catal Today* 1999;53:51–59.
21. Shah YT, Pandit AB, Moholkar VS. Cavitation Reaction Engineering. New York: Plenum Press/Kluwer Academic; 1999.
22. Storey BD, Szeri AJ. Water vapor, sonoluminescence and sonochemistry. *Proc R Soc Lond Ser A*. 2000;456:1685–1709.
23. Hart EJ, Henglein A. Sonochemistry of aqueous solutions: hydrogen-oxygen combustion in cavitation bubbles. *J Phys Chem*. 1987;91: 3654–3656.
24. Suslick KS. Sonochemistry. *Science* 1990;247:1439–1445.
25. Sivasankar T, Paunikar AW, Moholkar VS. Mechanistic approach to enhancement of the yield of a sonochemical reaction. *AIChE J*. 2007;53:1132–1143.
26. Frenklach M, Bowman T, Smith G, Gardiner B. Reaction rate coefficients. Gri-MechTM Website: http://www.me.berkeley.edu/gri-mech/ data/frames.html). Accessed January 2013.
27. Sivasankar T, Moholkar VS. Mechanistic approach to intensification of sonochemical degradation of phenol. *Chem Eng J*. 2009;49:57–69.
28. Sivasankar T, Moholkar VS. Physical insights into the sonochemical degradation of recalcitrant organic pollutants with cavitation bubble dynamics. *Ultrason Sonochem*. 2009;16:769–781.
29. Chakma S, Moholkar VS. Mechanistic features of ultrasonic desorption of aromatic pollutants. *Chem Eng J*. 2011;175:356–367.
30. Moholkar VS, Warmoeskerken MMCG, Ohl, CD, Prosperetti A. Mechanism of mass-transfer enhancement in textiles by ultrasound. *AIChE J*. 2004;50:58–64.
31. Krishnan JS, Dwivedi P, Moholkar VS. Numerical investigation into the chemistry induced by hydrodynamic cavitation. *Ind Eng Chem Res*. 2006;45:1493–1504.
32. Toegel R, Gompf B, Pecha R, Lohse D. Does water vapor prevent upscaling sonoluminescence? *Phys Rev Lett*. 2000;85:3165–3168.
33. Sivasankar T, Moholkar VS. Mechanistic features of the sonochemical degradation of organic pollutants. *AIChE J*. 2008;54:2206–2219.
34. Kumar KS, Moholkar VS. Conceptual design of a novel hydrodynamic cavitation reactor. *Chem Eng Sci*. 2007;62:2698–2711.
35. Keller JB, Miksis MJ. Bubble oscillations of large amplitude. *J Acoust Soc Am*. 1980;68:628–633.
36. Press WH, Teukolsky SA, Flannery BP, Vetterling WT. Numerical Recipes. New York: Cambridge University Press; 1992.
37. Chemical equilibrium calculation. Bioanalytical Microfluidics Program, Colorado State University Website. http://navier.engr.colostate.edu/∼dandy/code/code-4/index.html. Accessed January 2013.
38. Leighton TG. The Acoustic Bubble. San Diego: Academic Press; 1994.
39. Grossmann S, Hilgenfeldt S, Zomack M, Lohse D. Sound radiation of 3 MHz driven gas bubbles. *J Acoust Soc Am*. 1997;102:1223–1227.
40. Moholkar VS, Warmoeskerken MMCG. Integrated approach to optimization of an ultrasonic processor. *AIChE J*. 2003;49:2918–2932.
41. Hirschfelder JO, Curtiss CF, Bird RB. Molecular theory of gases and liquids. New York: Wiley, 1954.
42. Condon EU, Odishaw H. Handbook of Physics. New York: McGraw Hill; 1958.
43. Reid RC, Prausnitz JM, Poling BE. Properties of Gases and Liquids. New York: McGraw Hill; 1987.

Manuscript received Jan. 28, 2013, and revision received Apr. 16, 2013.